A GCM Study of the 1988 United States Drought

KINGTSE C. MO AND J. R. ZIMMERMAN

Climate Analysis Center, NMC/NWS/NOAA, Washington D.C.

E. KALNAY AND M. KANAMITSU

Development Division, NMC/NWS/NOAA, Washington, D.C.

(Manuscript received 12 March 1990, in final form 10 December 1990)

ABSTRACT

June 1988 has been classified as one of the hottest and driest months on record in the United States. This study used the NMC Medium-Range Forecast (MRF) T40 model to simulate circulation features of June 1988 and to investigate the relationship between sea surface temperature anomalies (SSTA) and circulation patterns in the Northern Hemisphere. Three control experiments have been performed using three different initial conditions, separated by one day (21, 22, and 23 May 1988) and using SSTA fixed at the starting date. The three forecasts, and their average, are remarkably skillful in the Northern Hemisphere. The observed anomaly of June 1988, a wave train with a persistent ridge in the north-central United States and a northward shifting of the jet stream in the Pacific–North America area, is very well simulated in each of the integrations. All three experiments were repeated using the same initial conditions, but with climatological SST. The wave train generated is similar to that in the control experiments, but it is not as robust. The simulated jet streams are also similar to those in the control experiments. Two experiments with the 1988 SSTA, but with initial conditions of 22 May 1987 and 22 May 1989 were also run. The circulation patterns generated by these runs are very different from those of 1988, indicating that the persistence of the anomalous ridge in the north-central United States after late May 1988 was not due to the SSTA of the May 1988 alone.

A barotropic analysis was done to obtain the normal modes associated with the 300-mb streamfunction of the June climatology. The analysis indicates the existence of a slowly growing mode with structure similar to the anomalies of 1988. This result, as well as the numerical experiments, suggests that the persistence of the June 1988 wave train may be associated with initial conditions, which were in a rather stable regime. The SSTA may have helped to strengthen the pattern, but the wave train associated with the 1988 drought could not have been generated by SSTA alone.

1. Introduction

The United States drought of 1988 was among the most severe in the Midwest of the past half century. The driest and hottest periods in over 90 years were recorded in parts of the Plains, the Midwest, and the lower Mississippi Valley. The severity of the Midwest drought peaked in June, but the development of the drought can be traced back one or more years in different parts of the country. In the beginning of July, normal rainfall returned to some parts of the central United States and improved short-term water deficiencies.

This drought was clearly associated with an unusual displacement of the jet stream, which was related to an upper-air ridge pattern over the north-central states and south-central Canada. Such a pattern deflected the rain bearing storms farther up to the north, away from the central United States (Ropelewski 1988).

Corresponding author address: Dr. Kingtse Mo, NOAA/NWS, W/NMC52, Washington, D.C. 20233.

Heat waves and droughts are part of the natural climate variability. They can also be influenced by anomalous boundary forcing, such as snow cover and sea surface temperatures (Namias 1982; Rasmusson 1987). They could also be caused by extreme dry soil conditions (Wolfson et al. 1987) and accumulation of warm temperatures over a long period of time before the drought.

For the 1988 drought, Trenberth et al. (1988) suggested that the sea surface temperature anomalies (SSTA) in the tropical Pacific were the main cause of the event. Their suggestion was based essentially on the results of simulations with a linear model. Linear models may not give a complete picture of this complicated relationship between tropical forcing and extratropical circulations, in which nonlinear terms are important and should not be ignored (Sardeshmukh and Hoskins 1988).

Palmer and Brankovic (1989) did GCM experiments using the ECMWF model to confirm that the SSTA were linked to this United States drought. However, their control experiment consisted of a single successful

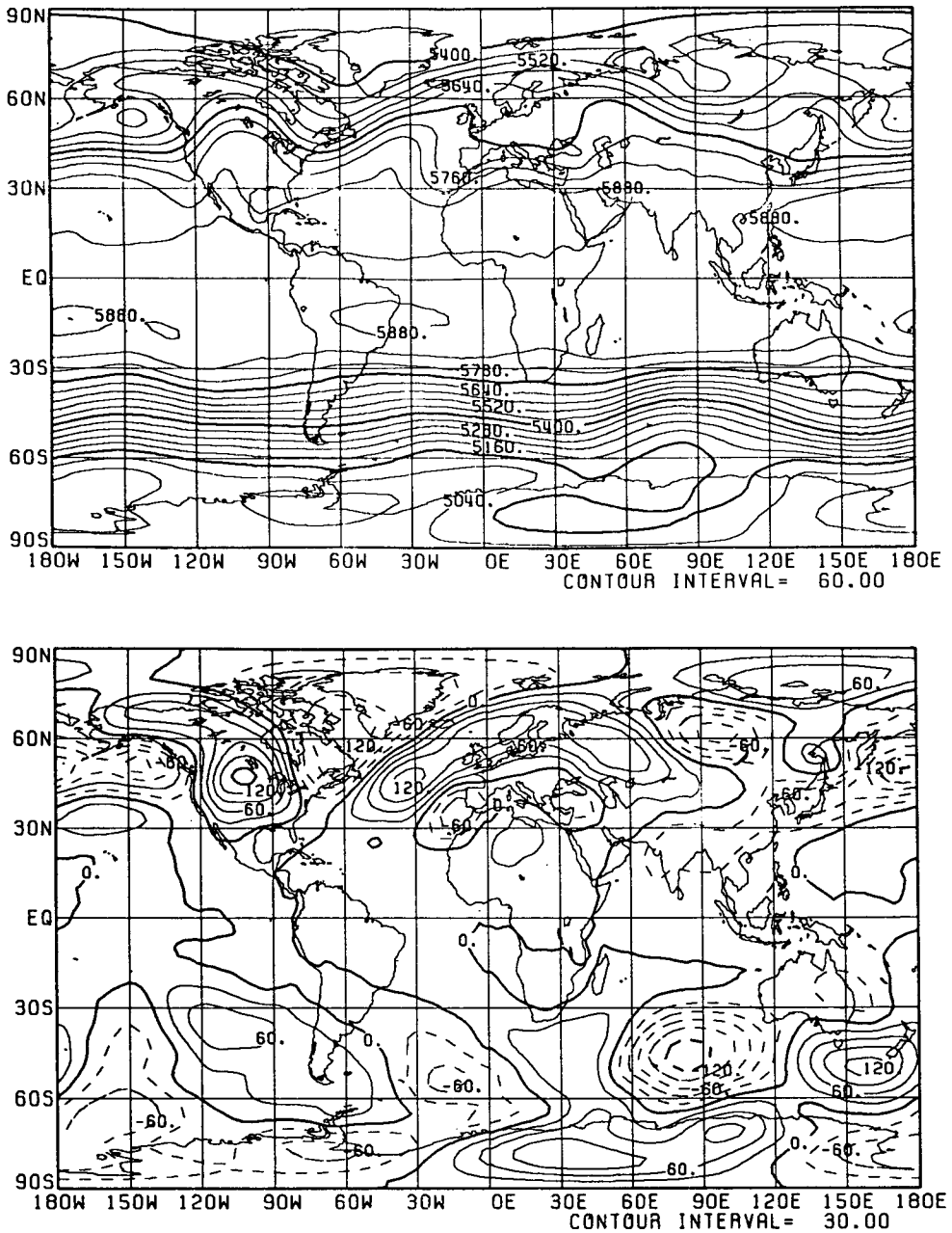

FIG. 1. (a) Monthly mean 500-mb geopotential height for June 1988 from NMC analyses; contour interval 60 m. (b) Same as (a), except for quasi-stationary waves; contour interval 30 m.

30-day forecast started on 22 May 1988, since a second 30-day forecast beginning one day earlier was much less skillful. Their conclusions were reached by comparing the control run with an experiment with the same 1988 initial conditions but with the 1987 SSTA. The 1988 wave train over the Pacific–North America region disappeared after changing from 1988 SSTA to 1987 SSTA. The summer of 1988 was marked by a cold ENSO event (Ropelewski 1988) and the 1987 summer coincided with a warm ENSO event (Arkin 1988). Circulation patterns in both 1987 and 1988 were influenced by these anomalous ENSO conditions. Anomalies during these two summers in the tropics and subtropics formed almost a mirror image of each other (Rasmusson and Mo 1988). Perhaps it is then not surprising that the ECMWF model responded strongly to such a large shift in the boundary forcing, and the wave train disappeared when the SST of 1987

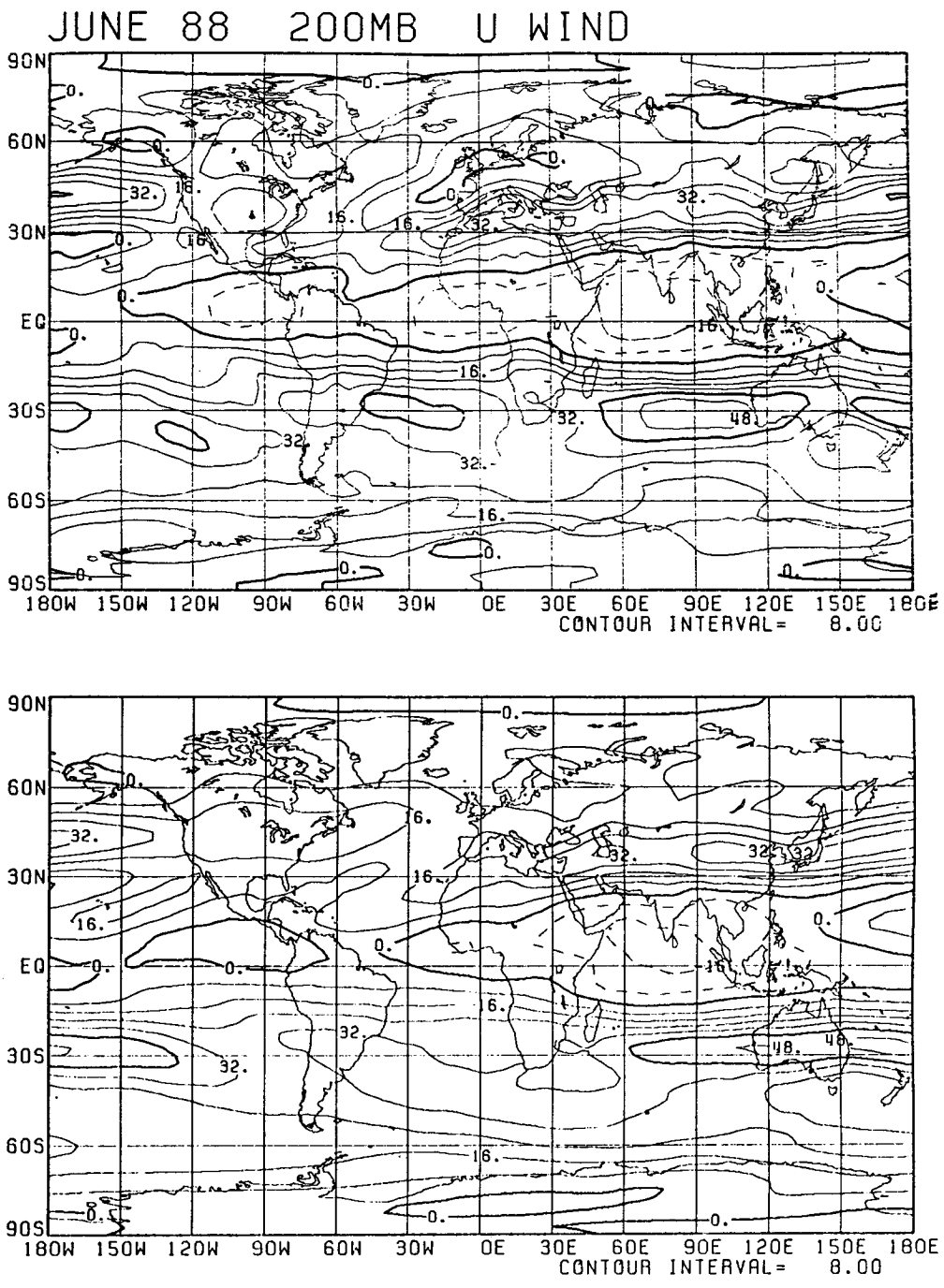

FIG. 2. (a) Monthly mean 200-mb zonal wind for June 1988 from NMC analysis; contour interval 8 m s^{-1}. (b) Same as (a), except for climatology.

was used. It should be noted that slight changes in the initial conditions (i.e., a run starting on 21 May 1988) also resulted in the disappearance of the drought pattern.

In this paper, the cause of the June 1988 drought is studied using the NMC Medium-Range Forecast (MRF) Model. By comparing experiments using the SSTA fixed at the starting dates and experiments from the same initial conditions but with climatological SST, we are able to assess the relative influences of SSTA and initial conditions on the atmospheric circulation. The circulation patterns of June 1988 are reviewed in section 2. Section 3 describes the model used and the results of the control experiments. Experiments using

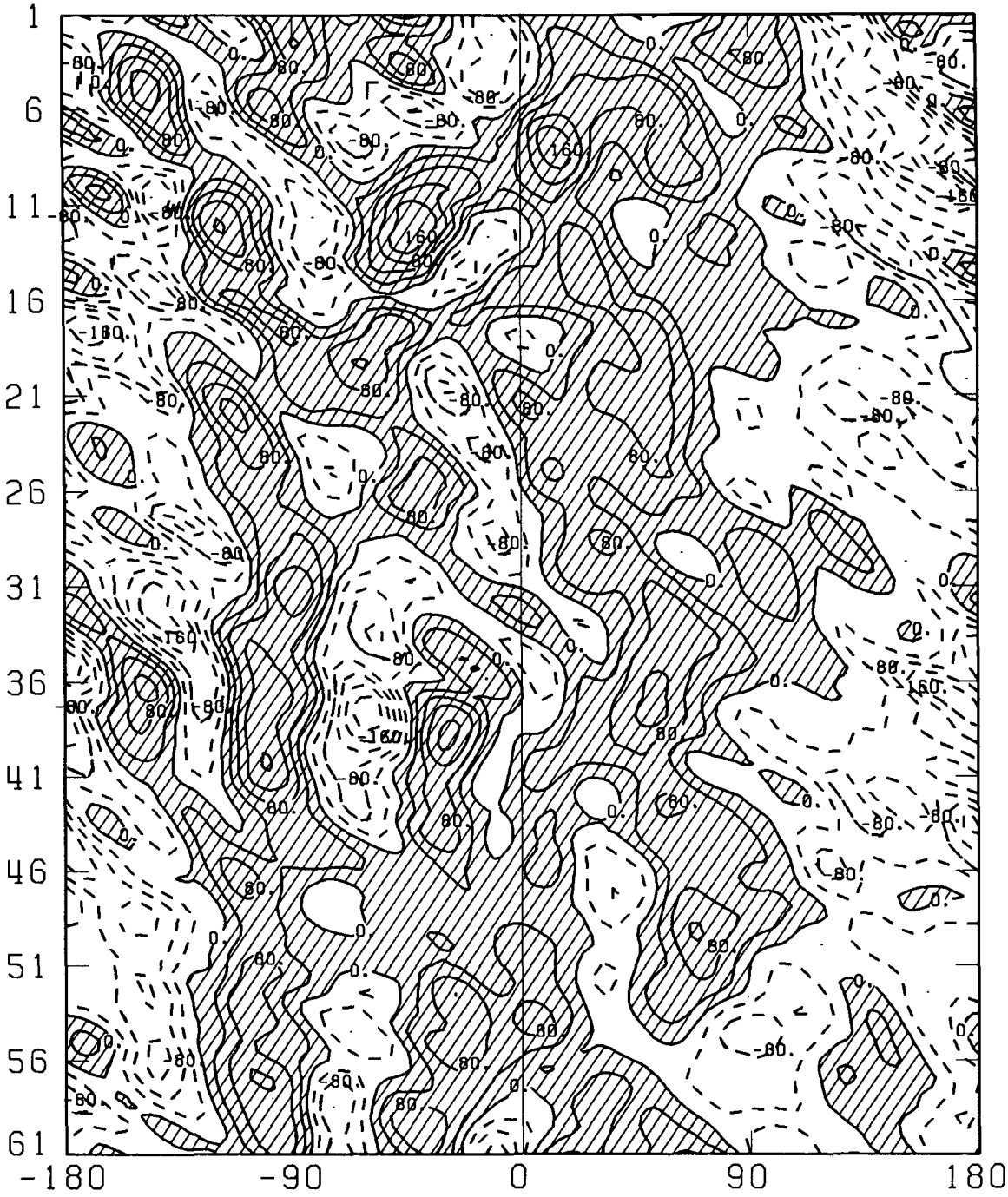

FIG. 3. Hovmöller diagram of quasi-stationary waves for 500-mb heights averaged over the latitude belt from 30° to 60°N for 1 May–30 June 1988. Positive values are shaded; contour interval 40 m.

climatological SST are presented in section 4. In section 5, we study the influence of the initial conditions on the simulations. A possible explanation of the persistent circulation pattern is that the initial conditions belong to a stable regime. This hypothesis is tested in section 6 using a barotropic model. Summary and conclusions are given in section 7.

2. Circulation features during June 1988

In this section, we review the anomalous atmospheric circulation and boundary conditions associated with the 1988 drought. All data presented here and the initial conditions for the model were derived from NMC analyses.

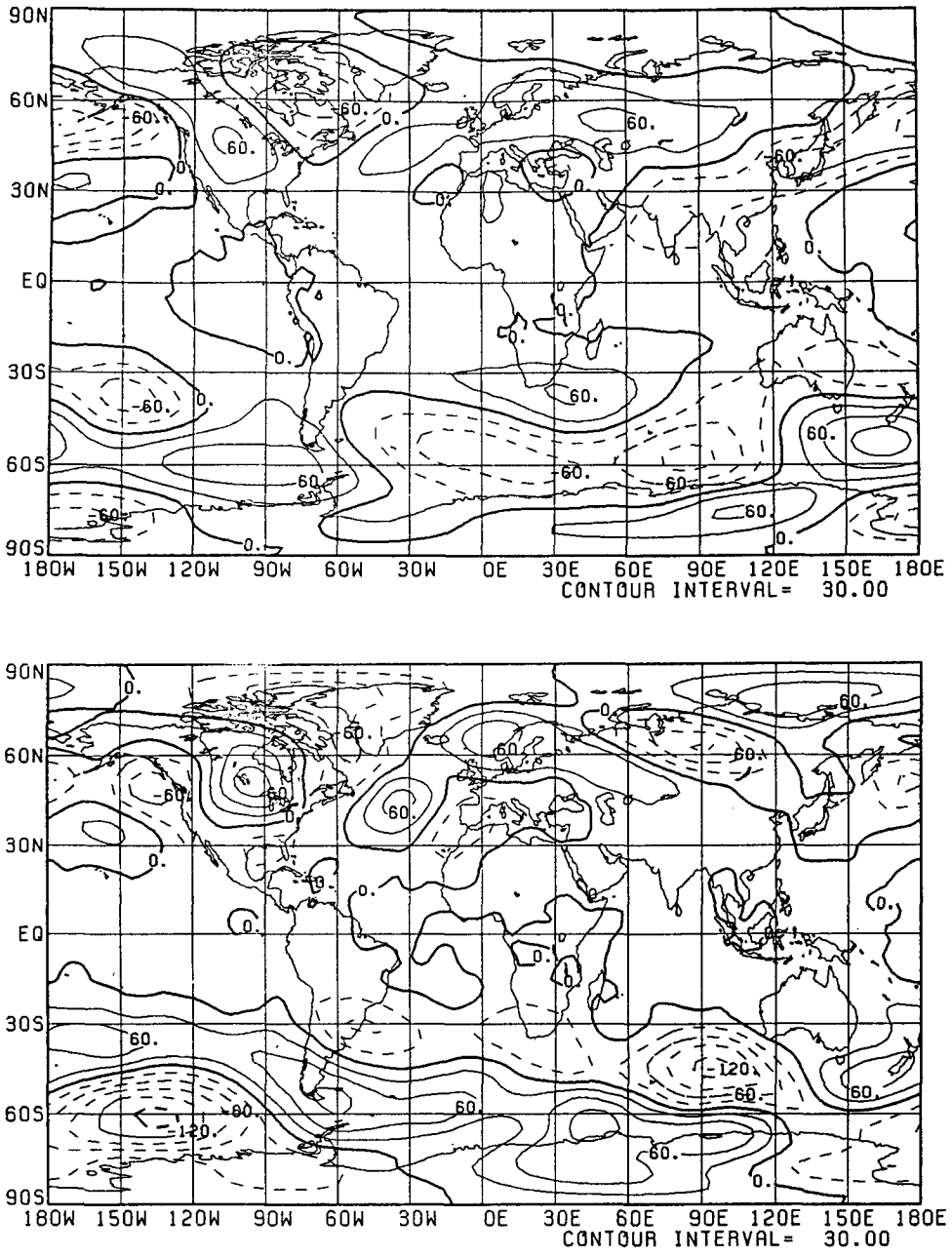

FIG. 4. (a) Standing waves for 500-mb heights for June climatology; contour interval 30 m. (b) Difference between quasi-stationary waves for 500-mb heights for June 1988 and June climatology; contour interval 30 m.

The heat wave and drought in the United States during 1988 were associated with a persistent anomalous upper-level circulation pattern during that period (Trenberth et al. 1988). Figure 1 shows the monthly mean 500-mb heights and quasi-stationary waves for June 1988, where the quasi-stationary wave component at a grid point is defined as the time-averaged departure of the value from the zonal mean at the same latitude. The chart shows a persistent ridge over the north-central states and central Canada, a trough extending from the Gulf of Alaska southward just west of the United States–Canadian coast, and a second trough along the east coast of North America. In the Southern Hemisphere (SH), a large area of positive height anomalies was located over the midlatitude eastern Pacific, and negative height anomalies were centered in the southern Indian Ocean. The jet stream, as indicated by the 200-mb zonal wind map of June 1988 (Fig. 2a) com-

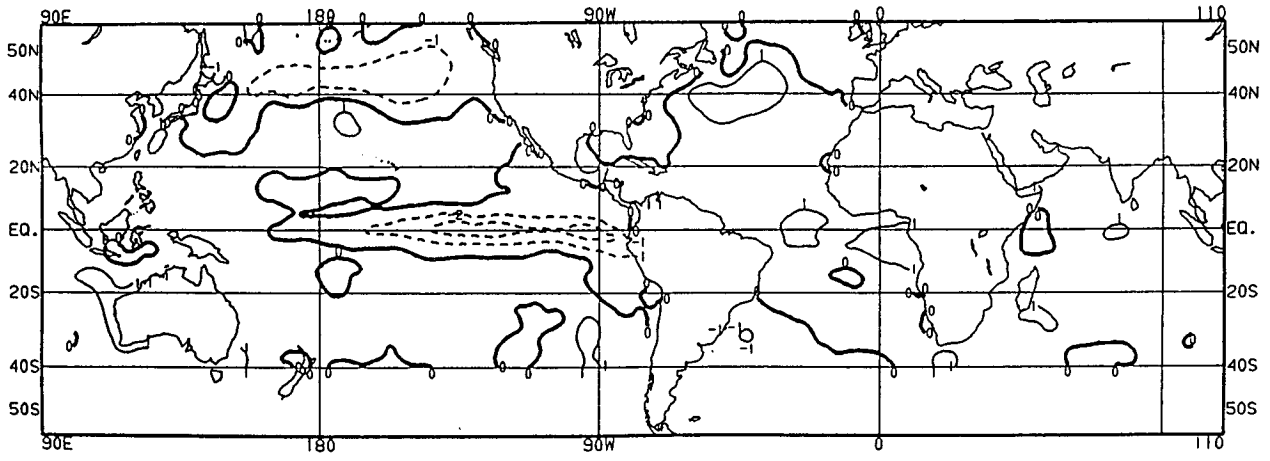

FIG. 5. Monthly mean sea surface temperature anomalies for June 1988; contour interval 1 K.

pared with the same map (Fig. 2b) for the 10-yr climatology, showed a northward displacement from the normal position near the United States–Canadian border. Storm tracks, which follow the axis of the jet, were displaced farther to the north during June 1988, and less than normal rainfall was recorded in the Midwest. As could be expected for a cold ENSO year, the equatorial Pacific easterlies were stronger than normal during June 1988. The subtropical jet in the SH was shifted to the Indian Ocean near Australia.

To show how persistent the Northern Hemisphere (NH) waves were throughout the summer of 1988, Fig. 3 presents a Hovmöller diagram (time–longitude cross section) for 500-mb zonally asymmetric component of the waves (departure from the zonal mean) averaged over 30°–60°N at each longitude from 1 May to 30 June 1988. A ridge moved from the Pacific Ocean to the central United States around 11 May. This feature was transient and shifted northward. Around 18 May, a ridge started to develop again over the central United States. Soon the wave-train pattern, with that ridge in the center and troughs in the Pacific near the west coast of the United States and east of Canada, started to form—around 21 May. The wave train reached its mature phase around 26 May and persisted during almost the entire month of June. The weak ridges in the Atlantic and Europe during June were less persistent. Elsewhere, circulation patterns varied from day to day.

The anomalous quasi-stationary waves in the NH during June 1988 represented a strong enhancement of the climatological stationary waves. Figure 4a gives the 500-mb stationary waves corresponding to the June climatology archived at the Climate Analysis Center, which covers the period from 1978–1988. Figure 4b gives the departure from climatology of the quasi-stationary waves during June 1988. The similarity between the two figures is striking: during June 1988 (Fig. 1b), the locations of highs and lows were the same as in climatology, but the magnitudes of the quasi-stationary waves for June 1988 were much stronger.

The June SST anomalies computed as departures

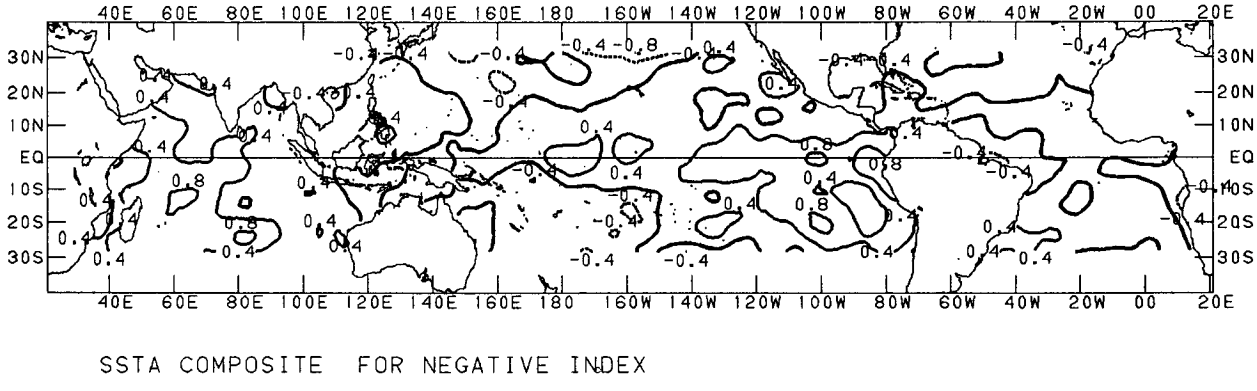

FIG. 6. Composite SST for 4 yr when the wave-train index was larger than one standard deviation; contour interval 0.4 K.

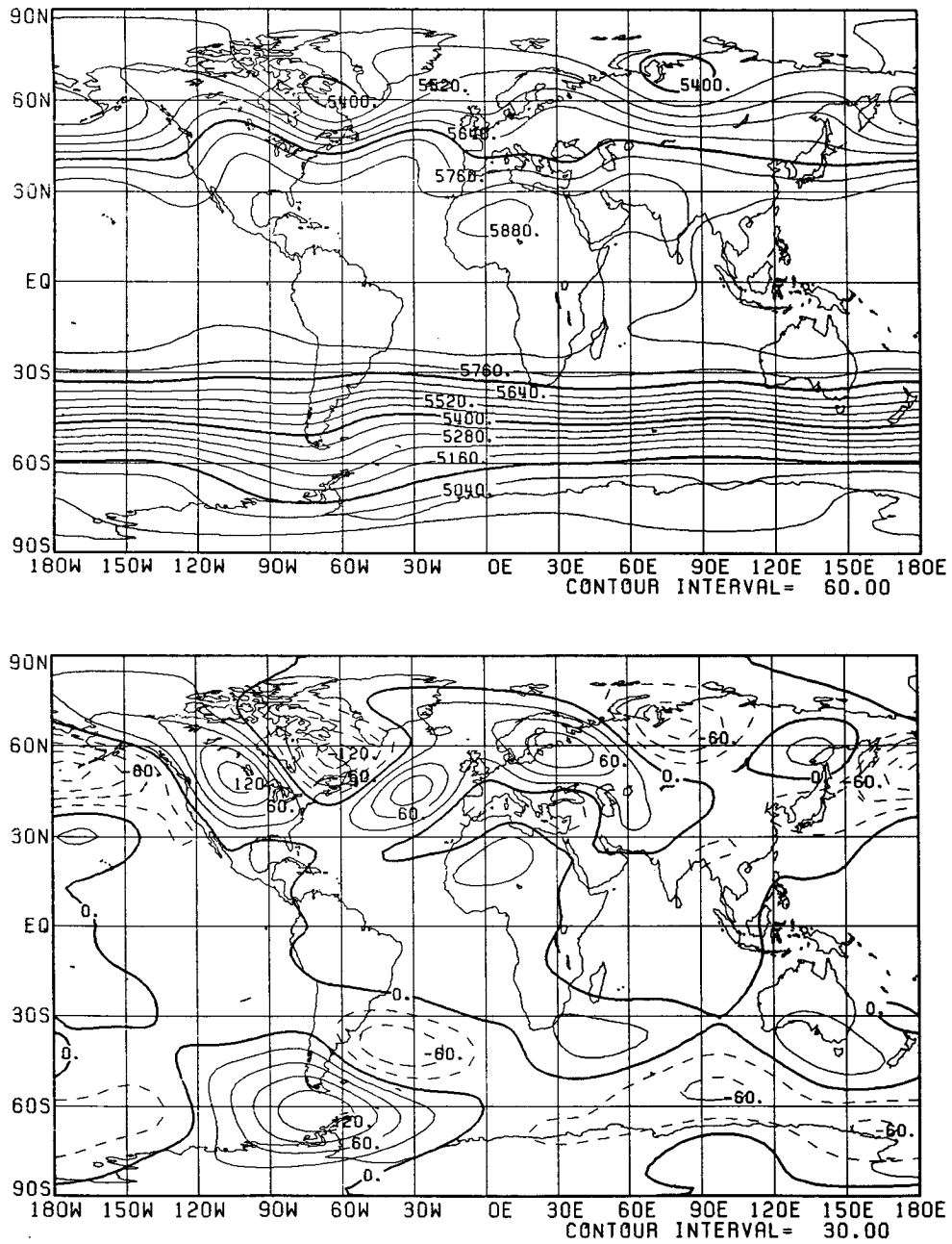

FIG. 7. (a) 30-day mean 500-mb heights averaged over three control experiments; contour interval 60 m. (b) Same as (a), except for quasi-stationary waves; contour interval 30 m. (c) 30-day mean 500-mb heights averaged over the period 22 May–21 June 1988 from NMC analyses; contour interval 60 m. (d) Same as (b), except for analyses; contour interval 30 m.

from the COADS/ICE climatology documented by Reynolds (1988) are given in Fig. 5. It shows typical features of a cold event with negative SSTA in the equatorial Pacific east of the date line. Negative SSTA are also found in the Pacific near 45°N.

Before performing the GCM study, we attempted to determine from historical data whether there is a teleconnection between the tropical SSTA and the 1988 wave-train pattern during June. For this purpose, we designed a "wave-train index." The same concept was used to describe heat waves in the United States (Wolfson and Atlas 1986). The dataset used was the monthly mean 700-mb heights archived from the Climate Analysis Center, which covers the period from 1949–

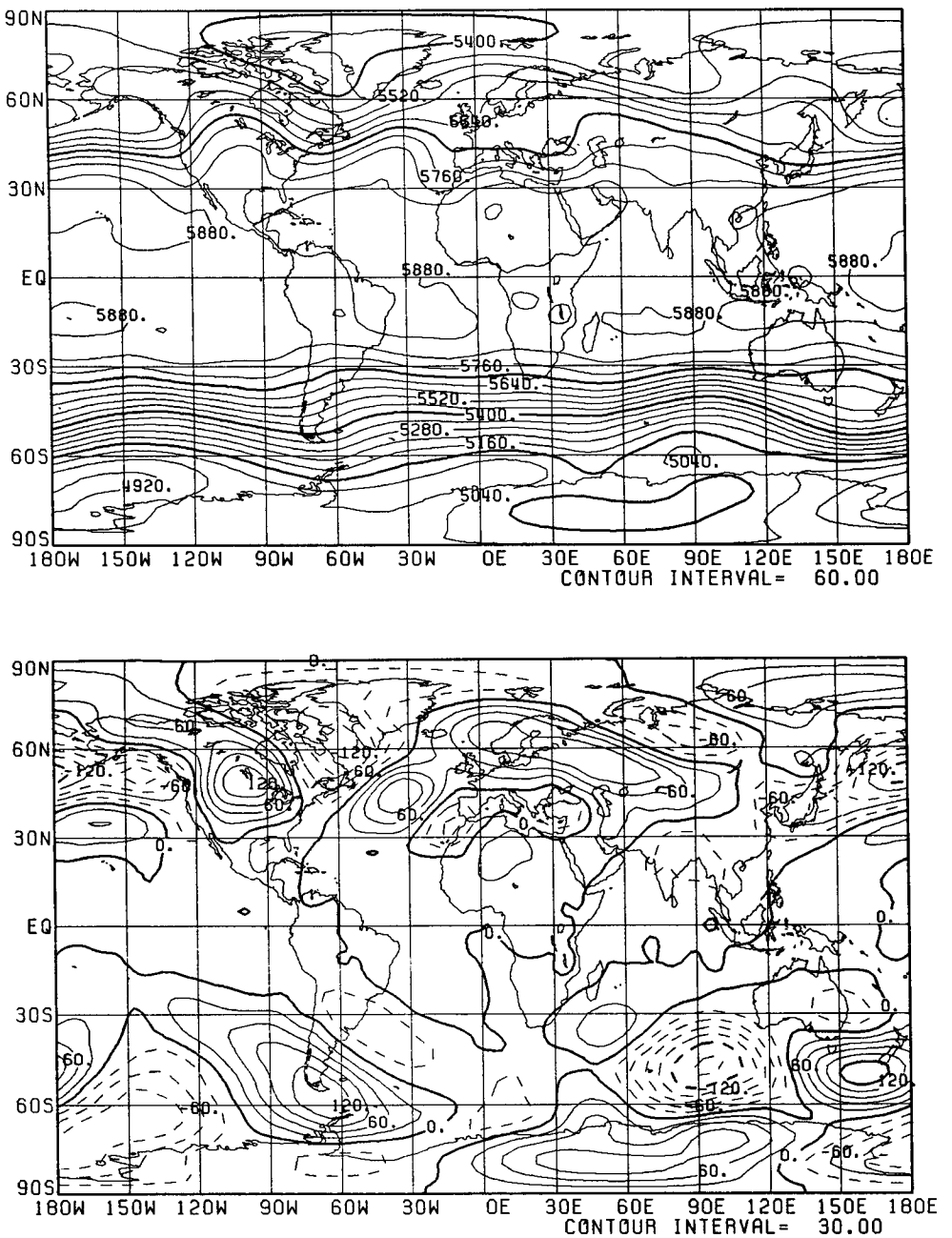

FIG. 7. (*Continued*)

1989. The index was computed using anomalies at the centers of highs and lows of the wave-train pattern of June 1988.

Index = $-Z'(50°N, 140°W) + Z'(50°N, 110°W) - Z'(60°N, 60°W) + Z'(50°N, 30°W)$, where Z' at each grid point is defined as the deviation from the 40-yr June climatology computed from the same dataset.

The wave-train index was computed for each June in the 40-yr data. Years when the wave index was greater than one standard deviation are 1961, 1970, 1972, 1983, 1986, and 1988. This list includes some ENSO warm events as well as some ENSO cold events, suggesting that this pattern may not be related to ENSO events. Figure 6 shows the composite SSTA for these selected years except 1988. The dataset used for the SSTA composite was the COADS data (Halpert and Ropelewski 1989). The composite SSTA are weak in the whole Pacific Ocean, and there is no resemblance between this composite and the SSTA of 1988. We also correlated the wave-train index and SSTA during

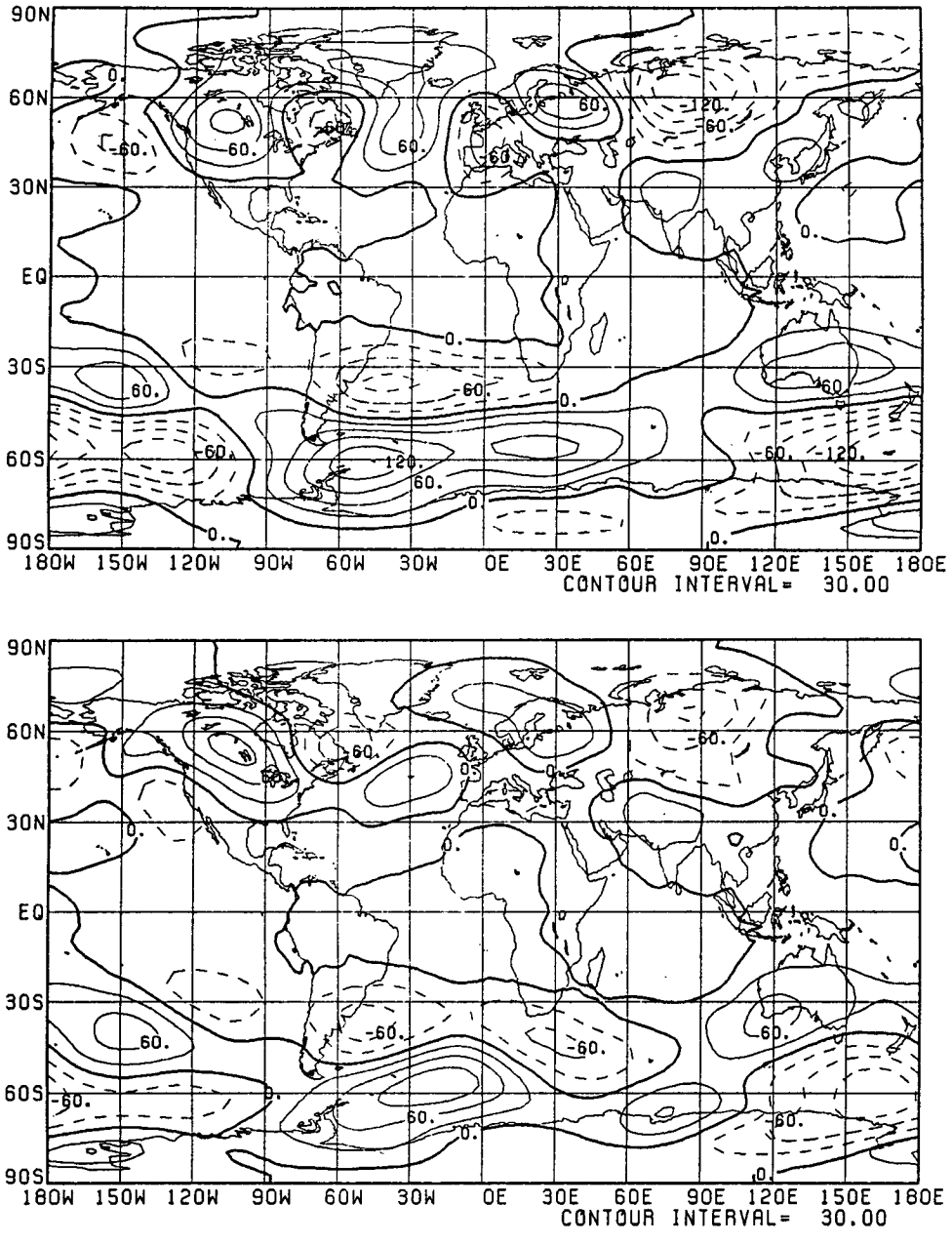

FIG. 8. (a) Difference map between the 30-day mean quasi-stationary waves for 500-mb heights for the control experiment with the initial conditions at 22 May 1988 and June climatology; contour interval is 30 m. (b) Same as (a), except for the 21 May 1988 initial conditions. (c) Same as (a), except for the 23 May 1988 initial conditions. (d) Same as (a), except for corresponding analyses.

June. Again we could not find any significant signal. The observational evidence, therefore, suggests that on the average there is no clear relationship between the wave-train pattern of 1988 and SSTA in the Pacific.

However, the atmosphere is intrinsically nonlinear. The response may depend on the entire configuration of the forcing field, instead of on some regional signal. For these reasons, we approach the problem by performing GCM experiments.

3. Control experiments

All numerical experiments were done using a model identical to the operational 1989 NMC spectral model (NMC Staff 1988), except for the horizontal resolution. We used a T40 version of the model, while T80 is used for daily MRF operation. A detailed description of the model and of a 1-yr integration can be found in Kanamitsu et al. (1989).

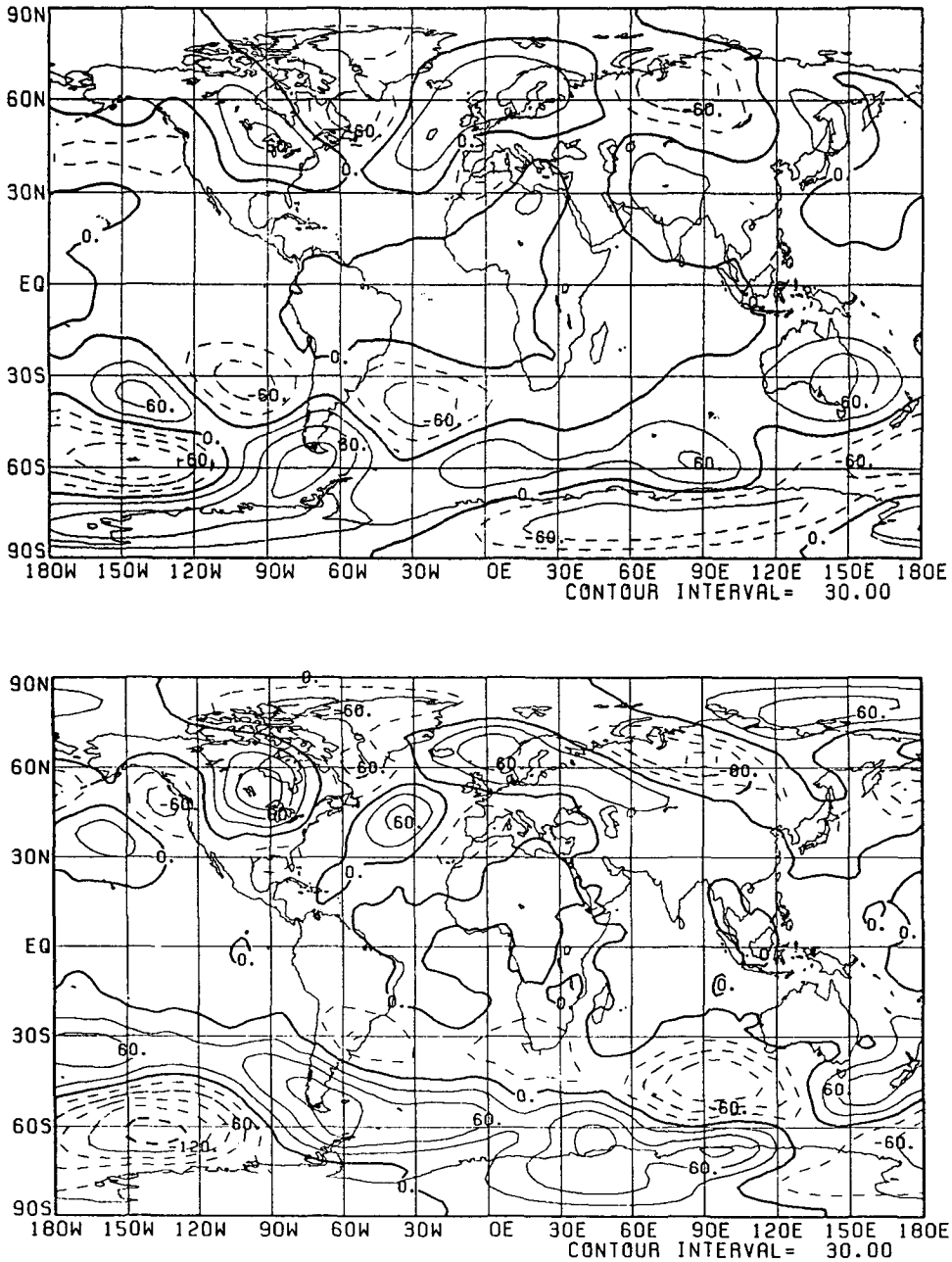

FIG. 8. (*Continued*)

Overall, the model climatology successfully reproduces 1000- and 500-mb heights and quasi-stationary waves in both hemispheres. The precipitation field is generally realistic, with good simulation of storm tracks, intertropical convergence zone (ITCZ), southern Pacific convergence zone (SPCZ), and monsoon. However, the center of maximum rainfall tends to shift from continents to the eastern shore. There is too little rain over Amazons and excessive rain over the Andes.

Since the wave train over North America became stationary near 25 May 1988, we made three 30-day integrations as control experiments starting from initial conditions of 21, 22, and 23 May 1988. The SST anomalies were fixed at the starting date during the entire integration for each experiment. The soil moisture field and snow cover were initialized with climatological values, but were calculated and updated by the model during the integration (NMC Staff 1988).

Figures 7a,b show the ensemble mean 500-mb heights and quasi-stationary waves for the three control

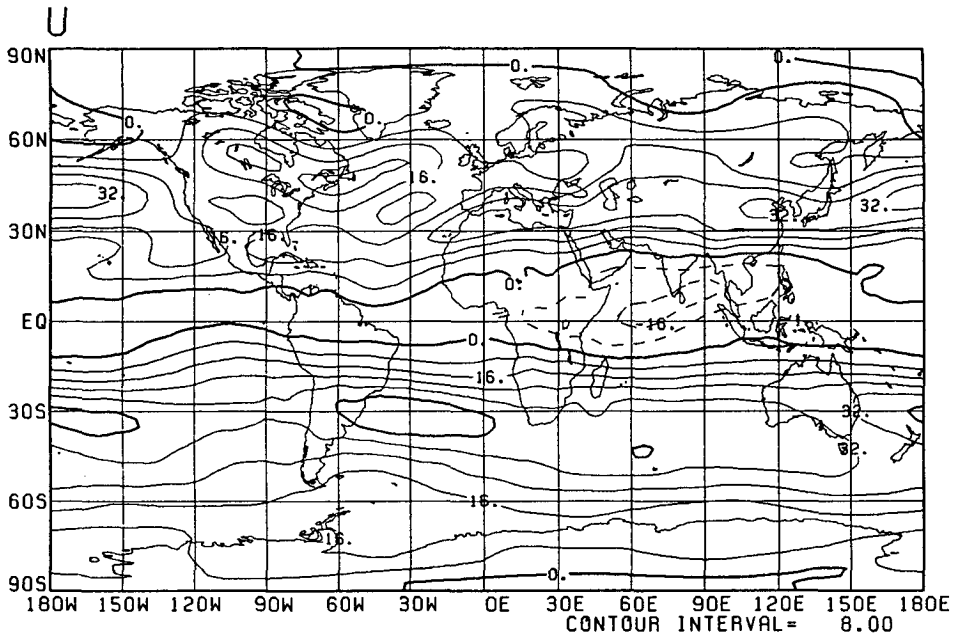

FIG. 9. 30-day mean 200-mb zonal wind averaged over three control experiments; contour interval 8 m s^{-1}.

runs, and the same plots from the corresponding period of analysis can be found in Figs. 7c,d. We show the global field to indicate general skill of forecasts. The agreement between simulated and observed heights is remarkably good in the NH. The wave train over North America is extremely well simulated both in location and strength. Even the features in Europe and Asia are also reproduced well. In the SH, simulated heights are more zonal than the observed field, but the ridge in the southern tip of South America is captured by the simulations. The simulated heights show the observed stationary waves in the Pacific, which are positive near

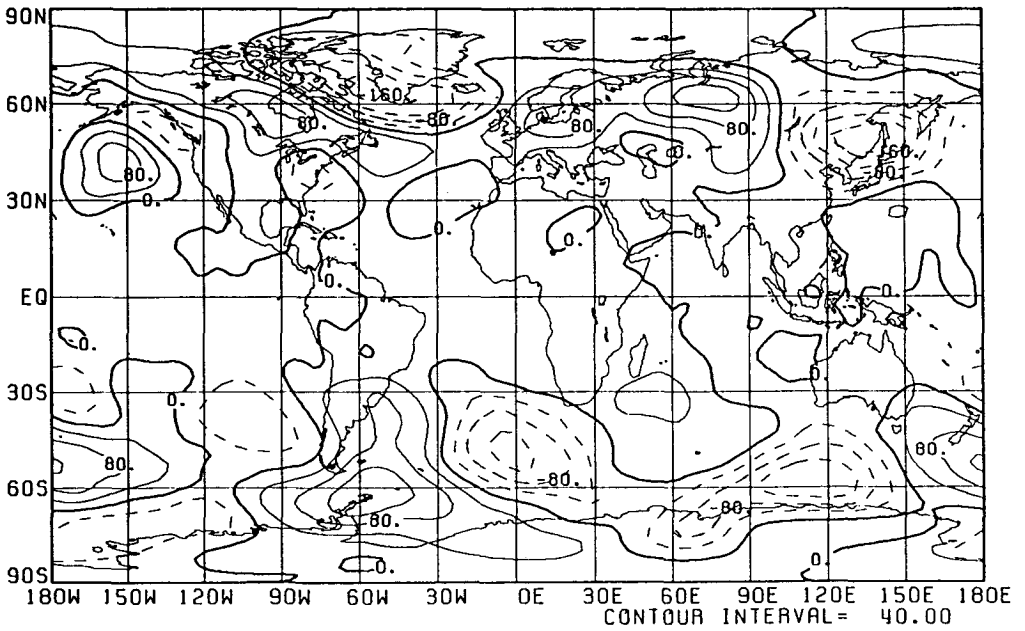

FIG. 10. Quasi-stationary waves for 500-mb heights averaged over the period 9–24 May 1988 from NMC analyses; contour interval 40 m.

50°S,160°E and negative near 90°E, but their magnitudes are strongly underestimated.

To assess the skill of the 1–30 day mean of these forecasts, we calculated the anomaly correlations and root-mean-square errors (rms) for each individual forecast and for the ensemble mean. Anomalies were defined as deviations from the June climatology. The anomaly correlation for the ensemble mean of the simulated 500-mb heights from 30° to 90°N is 0.60, and the rms error is 34.2 m compared with a climatological standard deviation of 54 m. If the regional area mean is included in the anomaly correlation, as in Miyakoda et al. (1986), the value increases to 0.71. For individual forecasts, the anomaly correlation varies from 0.41 to 0.65, and the rms error varies from 32 to 46.2 m. For 30-day summer forecasts, these are quite skillful. For comparison, Tracton et al. (1989) reported an average anomaly correlation of 0.39 for monthly forecasts during the NH winter of 1986–87. Monthly scores for the NH summer are lower, about 0.30. (Tracton, private communication). Values reported by ECMWF and UKMO are similar.

To show a better picture of the structure of the predicted anomalies, we plotted the differences between the simulated quasi-stationary waves and those in the June climatology for each experiment (Figs. 8a–c). Figure 8d shows the corresponding analyses. The agreement among the three anomaly forecasts is very good in the NH and less so in the SH. As indicated by Kistler et al. (1988) and Tracton et al. (1989), agreement among the members of an ensemble of forecasts can be used to estimate the skill of the forecast. The good agreement between the three forecasts of the June anomaly suggests that the predictions are reliable. We will return to this point in the next section.

Figure 9 shows the ensemble mean 200-mb zonal wind for the three control runs. The model successfully simulated the northward displacement of the westerlies over North America from its normal position. The Asian jet is also reproduced well. In the Southern Hemisphere, the subtropical jet in the Atlantic is captured by the simulations, but the local wind maximum in the Indian Ocean is entirely missing.

We examined the first and second 15-day means of each experiment. The wave train over North America appears in both 15-day means for all experiments (not shown). This indicates that the wave-train feature is not entirely due to persistence of the initial conditions during the first few days of the integration.

A purely persistence forecast (a 15-day average of the analysis previous to the initial conditions) is shown in Fig. 10. Such a forecast is rather poor: it does not show a ridge located in the United States. In addition, there is a high instead of a low center at the west coast of the United States. A shorter persistence forecast (e.g., 5-day mean) would be only marginally better over the United States.

4. Climatological SST (CSST) experiments

We performed the three 30-day integrations from the same initial conditions as control experiments but with climatological SST in order to examine the importance of SST anomalies to the circulation anomalies in 1988. Figure 11c shows the difference map for quasi-stationary waves in geopotential height at the 500-mb level for the NH from 30° to 90°N and June climatology. The overall pattern is very similar to the waves simulated in the control experiments (Fig. 11a), but there are some differences. The trough off the west coast of the United States is now located farther to the west and is also broader and weaker. The ridge in the north-central part of the United States is also weaker.

Several questions arise by these results: 1) are the wave trains simulated by both the control and CSST experiments significantly different from the June climatology?; and 2) are the differences between CSST experiments and control experiments statistically significant? Statistical t-tests were performed to address these questions.

From the three forecasts x_1, x_2, and x_3, we can define

$$t = \left| \frac{\bar{x}}{\sqrt{s/2}} \right|$$

where $\bar{x}$ is the mean departure from climatology and s is the variance. The value t needs to be over 4.3 and 2.92 for $\bar{x}$ to be statistically significantly different from zero at the 95% and 90% level, respectively.

Figures 11a and 11c show the corresponding t values for Figs. 11b and 11d, respectively. Areas where the ensemble mean of anomaly forecasts is significantly different from zero at the 95% level are shaded. Only areas north of 30°N are shown. For the control experiments, most centers of the wave train in the Pacific North America are statistically significant. The uncertainties are associated with the slight differences in the location of the centers of wave-train anomalies. For the CSST experiment, the negative anomalies centered on the west coast of the United States are no longer statistically significant. However, the ridge located in the north-central United States and central Canada, except the center of the ridge as well as the negative anomalies near the east coast of Canada, are still significant at the 95% level and are stronger than climatology. The center of the ridge shifts from one run to another and produces large variance and lower t value, but it is still significant at the 90% level. It is interesting that the statistically significant centers coincide almost without exception with the centers of well-predicted anomalies (cf. Fig. 4b). Even though this simple method to establish statistical significance in an ensemble of forecasts does not take into account the fact that grid points are not independent but belong to large-scale fields, it seems a promising way to highlight those areas where an ensemble forecast is reliable.

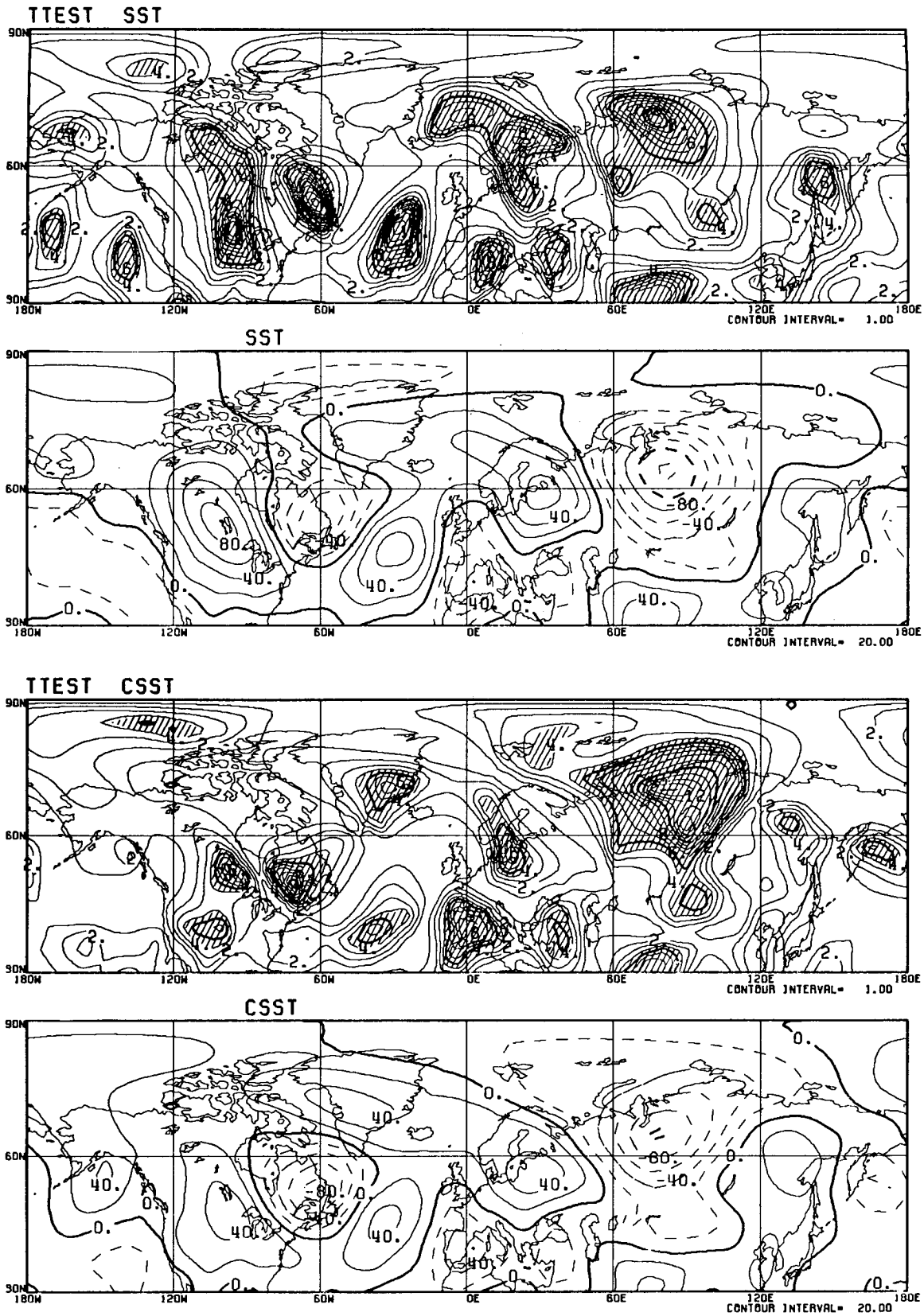

FIG. 11. (a) The corresponding t value for (b). Areas where features are statistically significant at the 95% level are shaded; contour interval 1.0. (b) Difference map between ensemble mean of quasi-stationary waves for 500-mb heights and June climatology for the control experiments; contour interval 20 m. (c) Same as (a), except for the CSST experiments. (d) Same as (b), except for the CSST experiments.

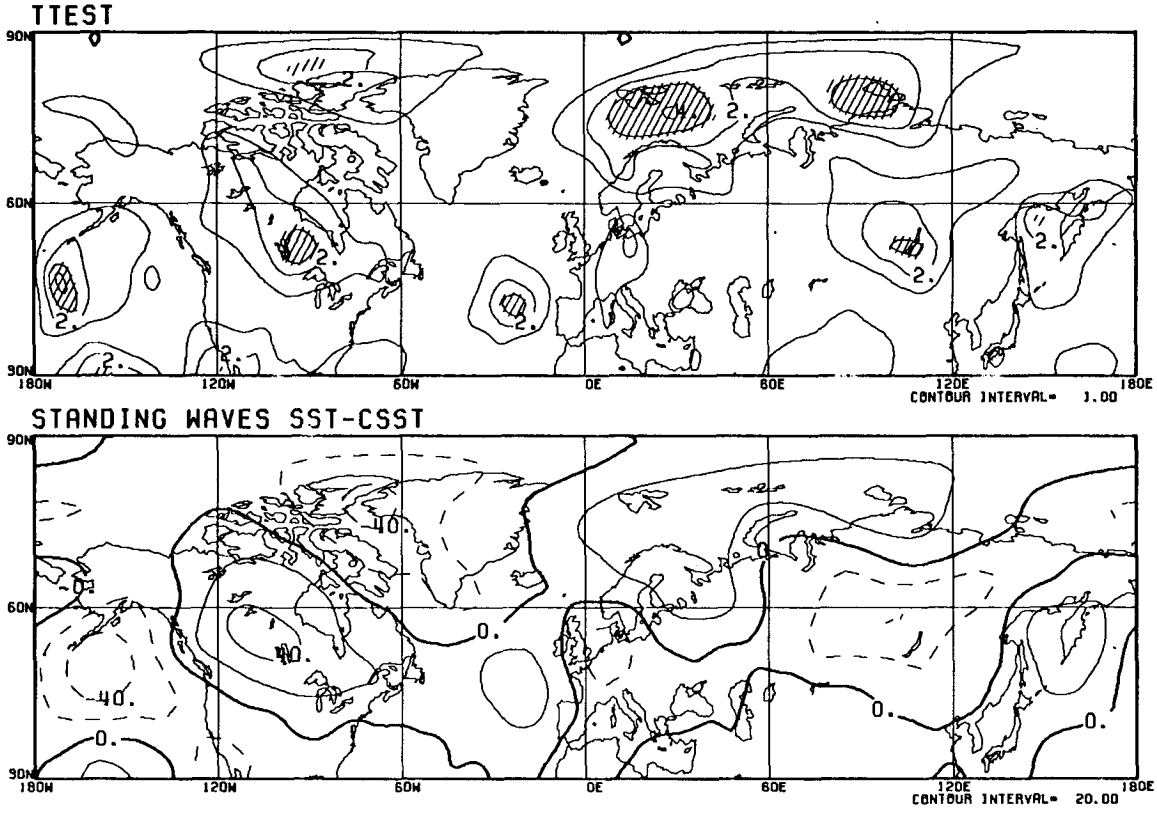

FIG. 11. (e) The corresponding t value for (f). Areas where features are statistically significant at the 95% level are shaded. (f) Difference map between ensemble mean of quasi-stationary waves for 500-mb heights for the control experiments and the CSST experiments.

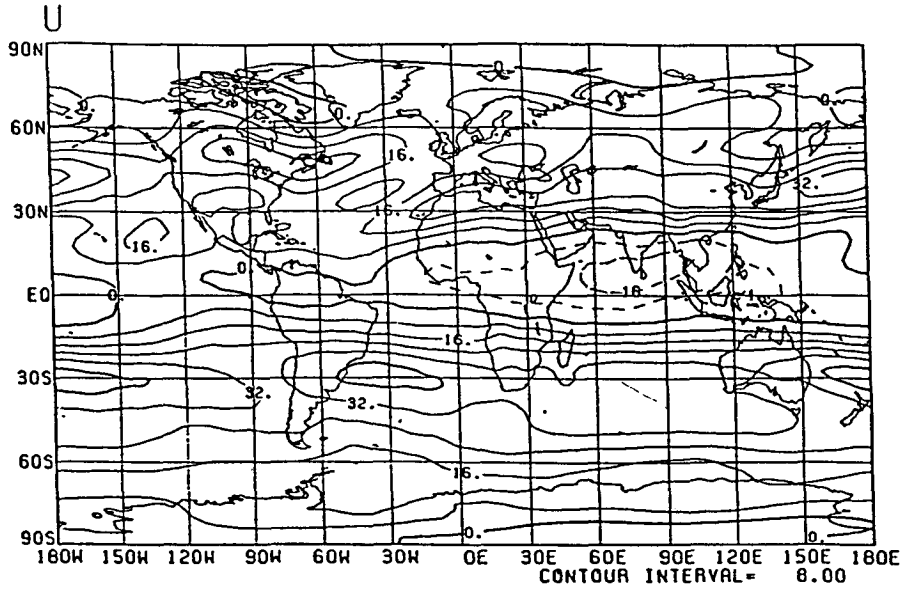

FIG. 12. Same as Fig. 9, except for CSST experiments.

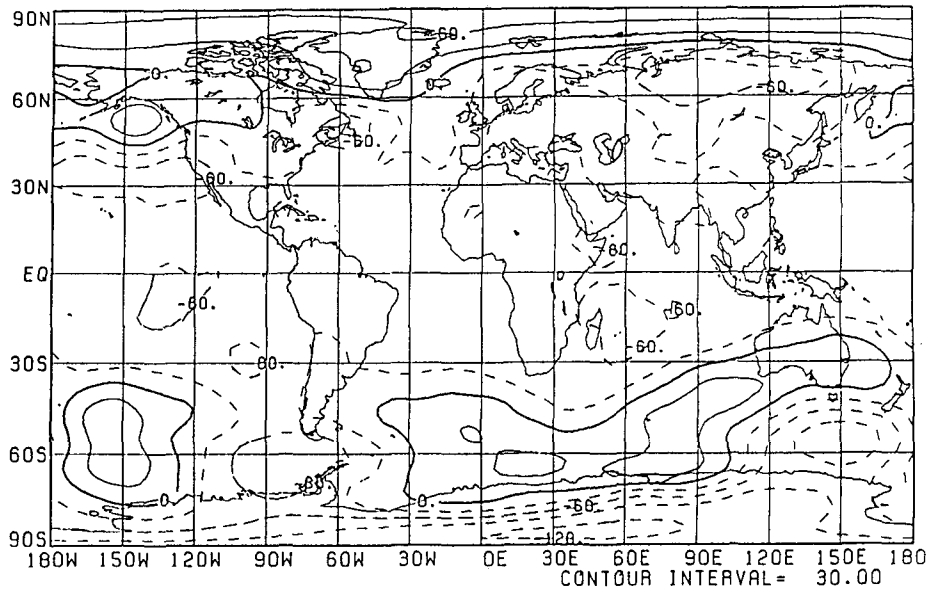

FIG. 13. Difference between 30-day mean quasi-stationary waves for 500-mb heights and June climatology averaged over six experiments with climatological SST and the initial conditions around 22 May 1987 and 22 May 1989; contour interval 30 m.

To consider the extent to which the SST anomalies have a significant impact on the forecasts, we now consider the difference map between the ensemble mean quasi-stationary waves at the 500 mb-level of the control and CSST experiments (Fig. 11f). The corresponding t value (Fig. 11e) is derived using the following procedure: we assume that the data follow the normal distribution. If x_1 and x_2 are the two sample means, and s_1 and s_2 are the variances for sample 1 and 2, then the value t is

$$t = \left| \frac{x_1 - x_2}{[(s_1 + s_2)/2]^{1/2}} \right| .$$

The difference between two sample means x_1 and x_2 is statistically significant at the 95% and 90% levels if t is larger than 2.78 and 2.13, respectively. The shaded areas in Fig. 11f indicate where differences are significant at the 95% level. The small size of the shaded areas indicates that the impact of SSTA was rather small. The weakening of the trough south of Alaska, the ridge over the central United States and Canada, and the trough over eastern Canada is only marginally significant. Only the changes over a small area near Hudson Bay are significant. This suggests that the SSTA's were not the only factor on the June 1988 circulation.

We have also examined the quasi-stationary waves of the first 15-day mean and the second 15-day mean for each of the CSST experiments. The wave train over North America is present during both halves of the periods, and only the center of the negative anomalies in the Pacific varies from one period to another. This suggests that the ridge in the central United States and Canada and the trough in eastern Canada are stable features that would have been present without the SST anomalies.

The 200-mb zonal wind ensemble mean for the CSST experiments (Fig. 12) differs little from that in the control experiments (Fig. 9). The westerlies over North America are still located north of their climatological position. The most noticeable change is the extension of the subtropical jet in the SH near Australia into the Pacific Ocean.

The results presented suggest that although the SSTA strengthened the wavetrain pattern in the NH, the shift of the jet stream and the persistent ridge over North America in these 30-day integrations starting from late May 1988 were not due to the SSTA alone. However, it is still possible that the initial conditions of 21–23 May were already influenced by the longer term presence of the cold ENSO event.

It is encouraging for dynamical extended range forecasting that the anomaly correlation for the area 30° to 90°N increased from 0.42 when climatological SST was used to 0.60 when the observed SST field was used. The rms error was also slightly worse with the climatological SSTA: 38 m for the CSST experiments compared to 34 m for the SSTA experiments.

Finally, we should consider whether the results of the experiments shown thus indicate true model skill coming from the initial and boundary conditions, or whether the model has a bias that tends to produce a summer wave train of stationary waves in phase with the June climatology stationary wave in all cases. If

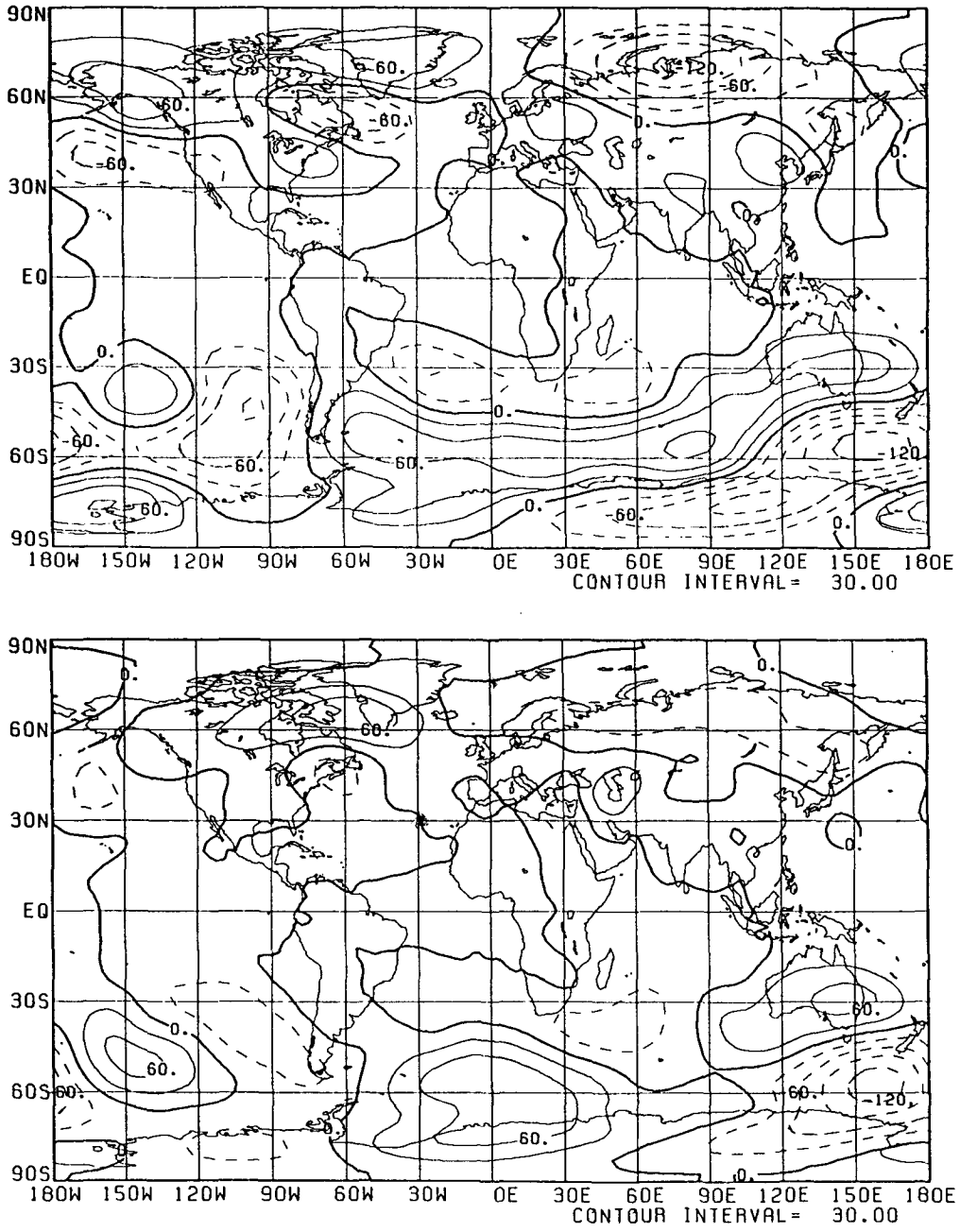

FIG. 14. (a) Difference between the 30-day mean quasi-stationary waves for 500-mb heights and June climatology for the experiment using the 1988 SSTA and the initial conditions at 22 May 1987; contour interval 30 m. (b) Same as (a), except for the experiment using 1988 SSTA and the initial conditions at 22 May 1989. (c) Difference between the 30-day mean quasi-stationary waves between an experiment using 1988 SSTA and climatological SST and the initial condition at 22 May 1987. (d) Same as (c), except for 1989. (e) The t value corresponding to (f). Areas where features are statistically significant at the 95% level are shaded; contour interval is 1.0. (f) Difference between the ensemble mean of 30-day means for three experiments with initial conditions at 22 May 1987, 1988, and 1989 with SSTA of 1988 and June climatology; contour interval is 20 m.

the model had such systematic errors, then the results for 1988 would be part of the model's climatology, i.e., they would show even if initial conditions from other years were used.

In order to test whether the 1988 forecasts had real skill, six additional integrations from 21–23 May 1987 and 22–24 May 1989 with climatological SSTs were performed. The resulting difference maps between the 30-day mean quasi-stationary waves for 500-mb heights averaged over six experiments and the June climatology are shown in Fig. 13. It is clear that the characteristic wave train over NH present in all of the 1988 integra-

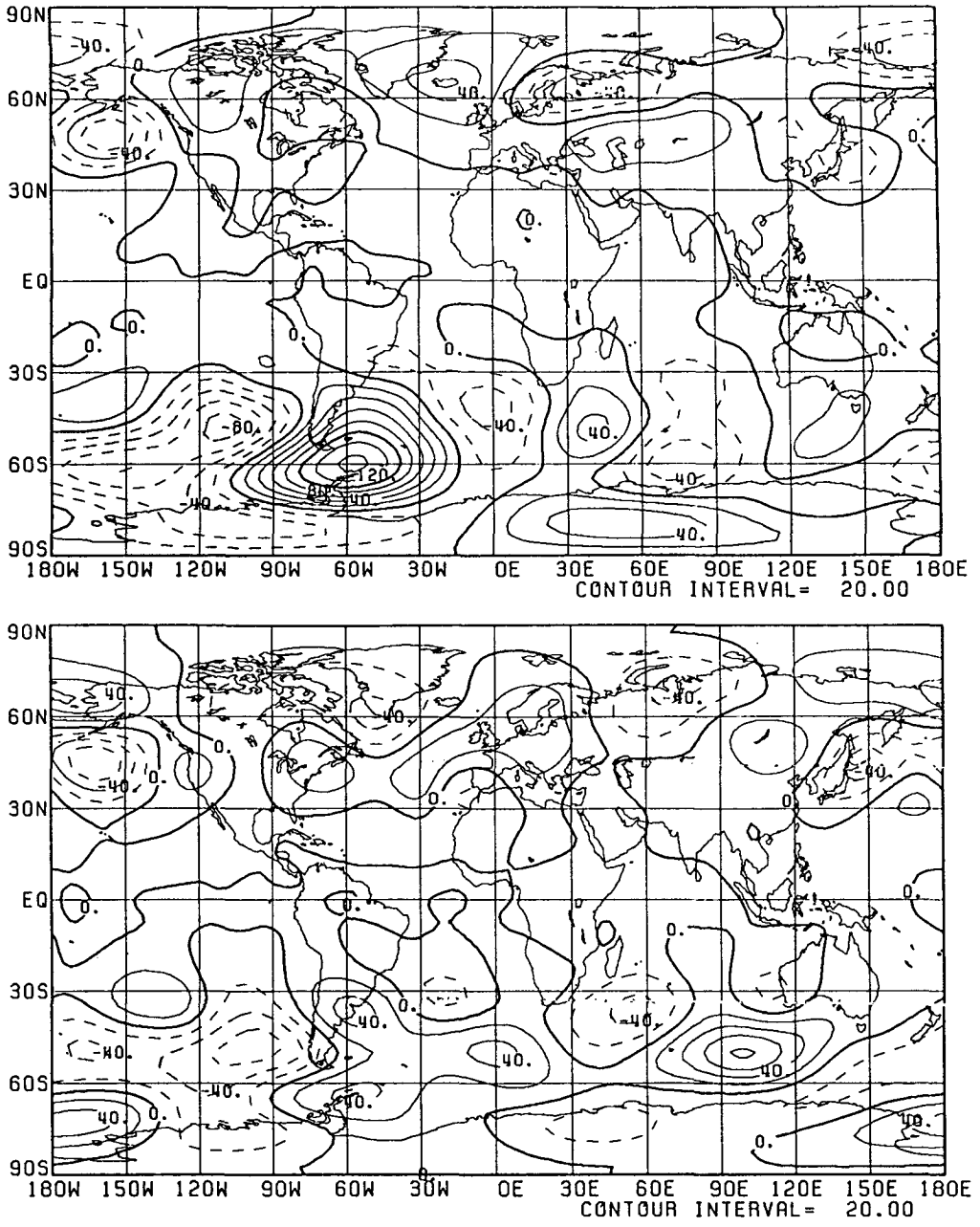

FIG. 14 (*Continued*)

tions is not apparent in either the 1987 or 1989 integrations.

From these experiments, we conclude that the wave-train pattern is not a part of the systematic error of the model, and the model is indeed able to simulate the features of 1988 circulation.

5. Other experiments using the 1988 SSTA

It is interesting to know which circulation features are clearly associated with the SSTA of 1988. We did two additional 30-day integrations with initial conditions at 22 May 1987 and 22 May 1989, but using the 1988 SSTA. These two experiments and the previous run with initial conditions at 22 May 1988 with 1988 SSTA will determine the circulation features associated with the 1988 SSTA.

Figures 14a and 14b show the difference between the 30-day mean 500-mb quasi-stationary wave and June climatology for forecasts with 22 May 1987 and 22 May 1989 initial conditions, respectively. It is clear that the wave-train pattern is not in the Pacific–North

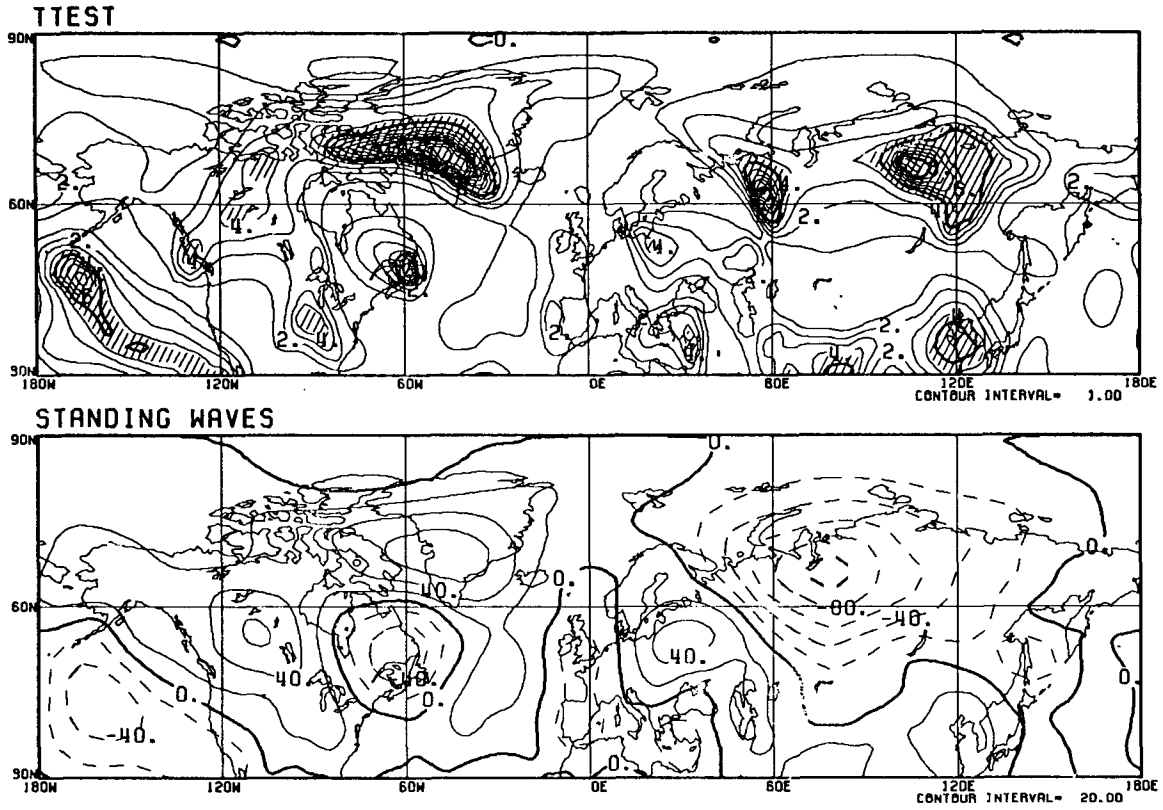

FIG. 14 (*Continued*)

America region for either the 1987 or 1989 case. We have also examined the first and second 15-day means for each experiment separately; the wave-train pattern cannot be found in both 15-day means of all experiments. We also plot the difference between Fig. 14a and the 30-day mean 500-mb quasi-stationary wave for the experiment with climatological SST but the same initial conditions in Fig. 14c. The same plot for the 1989 case is shown in Fig. 14d. It is apparent that the wave-train pattern is not part of the response to the 1988 SSTA.

To show the features associated with the 1988 SSTA, we plotted the difference map between the ensemble mean of the 30-day averaged 500-mb heights for three runs with initial conditions at 22 May 1987, 1988, and 1989 and with 1988 SSTA and the June climatology in Fig. 14f. The corresponding t value is given in Fig. 14e. The consistent features are the low located in the Pacific Ocean and the high centered near Greenland.

This set of experiments emphasizes the importance of the initial conditions. The features linked to the SSTA of 1988 may be the low center near the west coast of the United States and the high center near Greenland. Starting from initial conditions from other years, the SSTA of 1988 alone will not generate the strong ridge located over North America.

6. Barotropic instability

These experiments suggest that the May SSTA in the tropics were not the main cause of the June 1988 circulation anomalies. They also demonstrated the importance of the initial conditions in the maintenance of the wavetrain in the Pacific–North America region. Furthermore, we noticed the unusual similarity between the June climatology and the quasi-stationary waves for the 500-mb heights in June 1988. This similarity may suggest that this wave-train pattern belongs to one of the most dominant or stable regimes in the atmosphere and may be easily excited by disturbances, especially since a similar pattern has been obtained by forcing a linear model with idealized tropical heating and cooling (Trenberth et al. 1988). It is possible that the wave-train pattern may be associated with the barotropic instability of the climatological flow. As in the winter cases studied by Simmons et al. (1983), if this particular anomaly pattern resembles the normal mode structures, it may efficiently extract energy from the climatological mean flow. According to the study by Simmons et al. (1983), low-frequency transients associated with barotropic instability can also shift the jet streams and influence the storm tracks. These patterns are easily excitable by tropical forcing, although

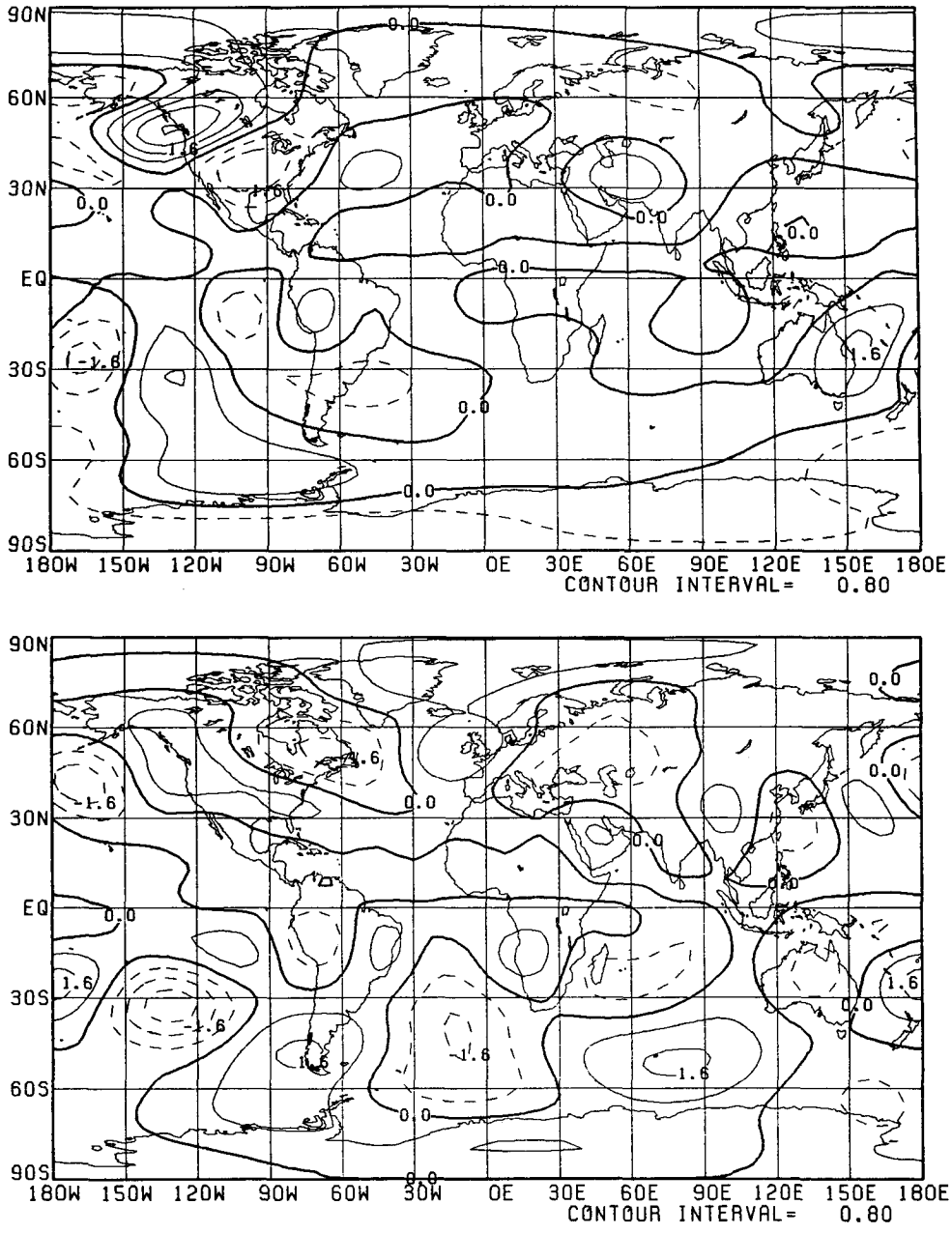

FIG. 15. (a) A and (b) B for the first normal mode simulated from a barotropic model. (Units: dimensionless.)

they are not very sensitive to the particular location of the heating.

To test this hypothesis, we derived the normal mode structures associated with barotropic instability of the climatological flow. The barotropic model used is based on that of Legras and Ghil (1987) but modified by Tribbia (private communication). It is a global spectral model and has a linear drag for dissipation, with a relaxation time of 15 days. A truncation at total wavenumber 21 (T21) was used to obtain the results presented here. The basic state used is the 300-mb climatological mean streamfunction for June. The calculation was repeated using the basic flow at the 200-mb level. There were minor changes in the growth rates and the frequencies of a particular mode, but with the same structures. The normal modes were obtained by solving the eigenfunction problem as outlined by Simmons et al. (1983). This gives us not only the fastest growing unstable mode, but also some modes with slightly slower growing rates. The results are given in the following form:

$$\exp(st)[A(x, y)\cos wt + B(x, y)\sin wt],$$

where s is the growth rate (inverse of the e-folding time)

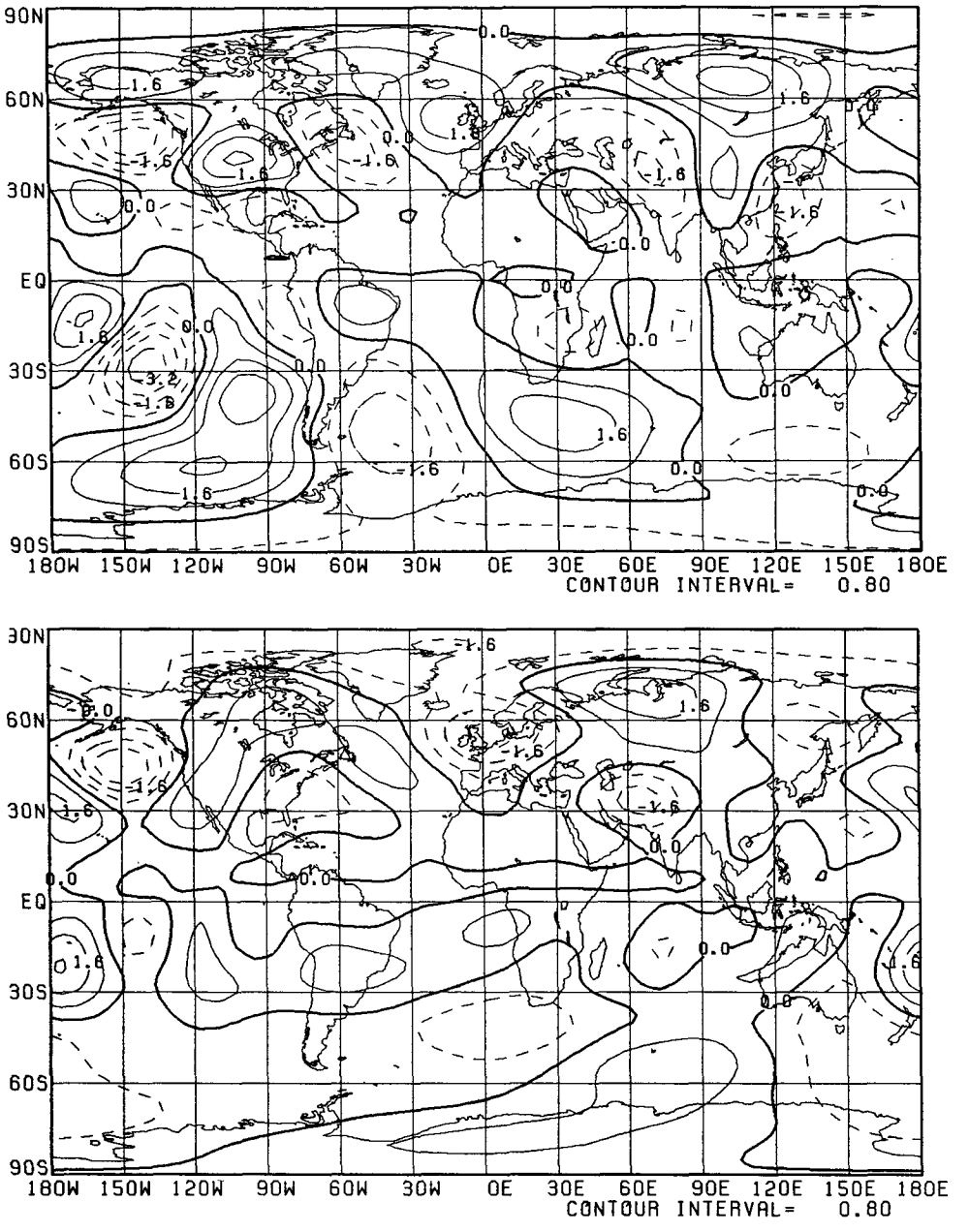

FIG. 16. Same as Fig. 15, but for the second normal mode.

and w is the frequency of the normal mode. The normal mode varies at any given time according to the structures and relative magnitudes of the function A and B modified by a growth factor.

The first mode has an e-folding time of 16.8 days and a period of 33.2 days. Structures A and B are shown in Fig. 15a and 15b, respectively. Much of the loading is concentrated in the Pacific, but the waves in the North American sector are not in phase with the wave-train pattern during June 1988.

The second mode has an e-folding time of 18 days and a period of 45.6 days. Structures A and B are shown in Fig. 16a and Fig. 16b. In the Pacific–North American region, the function A resembles the wave-train pattern of June 1988, especially the phase of the wave. Except for the low center near the east coast of the United States, the function B is weak and in phase with A. Over the Atlantic and Europe, the functions A and B are not in phase where amplitudes are large. This may be why only features in the Pacific region are more persistent and easily excited.

Although the mode associated with the June 1988 wave-train pattern is not the fastest growing mode, its period is the longest. If the initial states have a large

projection onto this mode, it will quickly respond to atmospheric forcing and will persist afterwards.

7. Discussion

We have performed GCM experiments to simulate the 1988 circulation anomalies and to study their cause. Control experiments were run, which include three 30-day integrations with SSTA fixed at the initial date and initial conditions for 21–23 May 1988. Northern Hemisphere forecasts, especially in the Pacific–North America region, are remarkably good.

The experiments were then repeated using the same initial conditions but with climatological SSTs. The resulting wave-train pattern over the Pacific–North America sector is weaker. Comparing to the control experiments, the strength of the ridge located in the north-central United States and Canada drops from 80 to 40 m, but is still stronger than June climatology. The simulated westerlies over North America are shifted northward and do not differ much from that of the control experiments. Nevertheless, the SSTA forecasts are more skillful, with $AC = 0.60$ compared with 0.42 for the CSST experiments. GCM experiments were also performed using 22 May 1987 and 1989 initial conditions with the SSTA of 1988. These fail to simulate the wavetrain pattern associated with the June 1988 circulation anomalies.

These experiments suggest that the persistence of the United States drought after late May 1988 was mainly due to a favorable initial configuration of the atmospheric anomalies. The effect of SSTA was much smaller than that of the initial conditions.

The wave-train pattern of June 1988 resembles the second fastest growing normal mode related to barotropic instability of the 300-mb climatological June flow. This mode is also the one with the longest period (45.6 days). Therefore, once it is excited into the initial conditions (possibly due to the influence of SSTA during the previous months), it will tend to persist longer as observed.

These conclusions are based on 30-day GCM experiments. We cannot overrule the influence of other oceanic or atmospheric forcing with time scales longer than one month on the atmospheric anomalies during the summer of 1988. It is possible that the low-frequency ENSO conditions or the long-term drought over the western and north-central regions of the United States created favorable initial conditions responsible for the circulation anomalies during 1988. This could not be easily tested, because it would require performing large ensembles of 90-day or longer forecasts. Findings in this paper may not be generalized to cover other heat wave and drought events in the United States. For the 1980 heat wave in the United States, a GCM study by Wolfson et al. (1987) indicated that initial conditions were important, but anomalous SSTA and soil moisture also had an impact at extended ranges.

Acknowledgments. We are grateful to Dr. Joseph Tribbia for his computer program to compute normal modes and his help in its implementation. We would like to thank Drs. Steven Tracton, Carlos R. Mechoso, and Eugene Rasmusson for their comments.

REFERENCES

Arkin, P. A., 1988: The global climate for June–August 1987: Mature phase of an ENSO warm episode persists. *J. Climate,* **1,** 306–324.

Halpert, S. M., and C. F. Ropelewski, 1989: Atlas of tropical sea surface temperature and surface winds. *NOAA Altas No. 8,* Department of Commerce, NOAA, Silver Spring, MD 20910, 223 pp.

Kanamitsu, M., K. C. Mo and E. Kalnay, 1989: Annual cycle integration of the NMC Medium Range Forecasting Model. *Mon. Wea. Rev.,* **119,** 2543–2567.

Kistler, R. E., E. Kalnay and M. S. Tracton, 1988: Forecast agreement, persistence, and forecast skill. Preprints, *Eighth Conf. on Numerical Weather Prediction,* Baltimore, Amer. Meteor. Soc. 641–646.

Legras, B., and M. Ghil, 1985: Persistent anomalies, blocking, and variations in atmospheric predictability. *J. Atmos. Sci.,* **43,** 433–471.

Miyakoda, K., J. Sirutis and J. Ploshay, 1986: One-month forecast experiments—without anomaly boundary forcings. *Mon. Wea. Rev.,* **114,** 2363–2401.

Namias, J., 1982: Anatomy of Great Plains protracted heat waves especially the 1980 United States summer drought. *Mon. Wea. Rev.,* **110,** 824–838.

National Meteorological Center Staff, 1988: Documentation of the research version of the NMC medium range forecasting model, 324 pp. [Available from the NOAA/NMC Development Division, Washington, D.C. 20233.]

Palmer, T. N., and C. Brankovic, 1989: The 1988 United States drought linked to anomalous sea surface temperature. *Nature,* **338,** 54–57.

Rasmusson, E. M., 1987: The prediction of drought: A meteorological perspective. *Endeavour,* **11,** 175–182.

——, and K. Mo, 1988: Vorticity budget of the upper tropical troposphere as evaluated from NMC analyses. *Proc. of the Thirteenth Annual Climate Diagnostic Workshop,* Boston, 265–268.

Reynolds, R. W., 1988: A real-time global sea surface temperature analysis. *J. Climate,* **1,** 75–86.

Ropelewski, C. F., 1988: The global climate for June–August 1988: A swing to the positive phase of the Southern Oscillation: Drought in the United States and abundant rain in monsoon areas. *J. Climate,* **1,** 306–324.

Sardeshmukh, P. D., and B. J. Hoskins, 1988: Generation of global rotational flow by steady idealized tropical divergence. *J. Atmos. Sci.,* **45,** 1228–1252.

Simmons, A. J., J. M. Wallace and G. W. Branstator, 1983: Barotropic wave propagation and instability and atmospheric teleconnection patterns. *J. Atmos. Sci.,* **35,** 414–432.

Tracton, M. S., K. C. Mo, W. Chen, E. Kalnay, R. Kistler and G. White, 1989: Dynamical extended range forecasting (DERF) at the National Meteorological Center. *Mon. Wea. Rev.,* **117,** 1604–1635.

Trenberth, K. E., G. W. Branstator and P. A. Arkin, 1988: Origins of the 1988 North American drought. *Science,* **242,** 1640–1645.

Wolfson, N., and R. Atlas, 1986: A simple diagnostic tool for the investigation of persistent phenomena with application to the summer 1980 heat wave. *Atmosphere: Atmos.-Ocean,* **24,** 111–127.

——, —— and Y. C. Sud, 1987: Numerical experiments related to the summer 1980 heat wave. *Mon. Wea. Rev.,* **115,** 1345–1357.